



## A Low Voltage BJT-Based Temperature Sensor with Duty Cycle Modulated Output with FOM Resolution of about 1.4pJ. °C<sup>2</sup> and Inaccuracy of ±0.11 °C (3σ) from -55 °C to 130 °C

Mohtaram Dehban Rahimabad <sup>a,\*</sup>, Ali Heidari <sup>a</sup>

<sup>a</sup> Department of Electrical Engineering, University of Guilan, Rasht, Iran

### ARTICLE INFO

#### Article history:

Received 15 July 2025

Received in revised form 13 August 2025

Accepted 18 August 2025

Available online 18 August 2025

#### Keywords:

CMOS temperature sensor

Duty-cycle

BJT

Low voltage

Resolution

### ABSTRACT

This paper presents a low voltage BJT-based smart temperature sensor with duty cycle modulated output and inaccuracy of ±0.11 °C (3σ) and FOM resolution of about 1.4pJ. °C<sup>2</sup> from -55°C to 130°C. This sensor can work with a supply voltage of 1.5V. It uses a BJT-based front-end to generate a proportional to absolute temperature voltage (V<sub>PTAT</sub>) and a complementary to absolute temperature voltage (V<sub>CTAT</sub>), which are then modulated to a duty-cycle output. Adding an integrator before the Schmitt trigger has increased the range of input changes of the Schmitt trigger. As a result, the hysteresis of the Schmitt trigger can be increased and it has better noise immunity. Implemented in a standard 0.18-μm CMOS process, the sensor has an active area of about 0.64mm<sup>2</sup> and can work with 1.5V from -55°C to 130°C with an inaccuracy of ±0.11°C (3σ). Power consumption is about 45uW.

## 1. Introduction

The precise monitoring of temperature over an extended range is a fundamental requirement in numerous modern electronic systems, particularly in fields such as environmental sensing, biomedical devices, and industrial automation. Achieving high accuracy in temperature measurement is vital to ensure system reliability, efficiency, and safety. However, alongside accuracy, energy efficiency has become a key design constraint due to the widespread use of battery-powered systems and energy-harvesting technologies, which often impose stringent power budgets [1], [2].

To meet these performance and energy demands, smart temperature sensors based on complementary metal-oxide-semiconductor (CMOS) technology have attracted significant

\* Corresponding author.

E-mail addresses: [s.dehban@yahoo.com](mailto:s.dehban@yahoo.com) (M. Dehban Rahimabad)

attention. These sensors typically integrate a temperature-sensitive core with a signal readout mechanism within a compact footprint. CMOS technology enables the co-integration of sensing elements with on-chip signal processing circuitry, which is crucial for applications requiring scalability and cost-effectiveness.

A variety of devices within standard CMOS processes can function as temperature-sensing elements. Common examples include bipolar junction transistors (BJTs), metal-oxide-semiconductor field-effect transistors (MOSFETs), and resistive components [3]. Among these, BJT-based temperature sensors are particularly well-regarded for their capability to deliver high accuracy and stability across a wide temperature spectrum [4], [5]. The analog signals generated by these sensing elements must be converted into digital form for further processing and communication. This can be achieved using several types of converters, such as analog-to-digital converters (ADCs) [6], time-to-digital converters (TDCs) [7], and frequency-to-digital converters (FDCs) [8], each offering trade-offs in terms of resolution, area, and power consumption.

In addition to traditional digitization techniques, encoding temperature information into a duty-cycle-modulated (DCM) signal has become an appealing approach, particularly in industrial applications. This method provides a simple yet robust interface that seamlessly integrates with both digital systems, such as microcontrollers and embedded processors, and analog control systems like thermostats [7]. The DCM format also lends itself to efficient transmission over noisy channels, contributing to its practicality in real-world scenarios.

As smart systems continue to evolve and operate in increasingly complex and noisy environments, the need for temperature sensors with enhanced noise immunity has become more critical than ever. Designing sensors that maintain high performance under such conditions is essential to ensure the reliability and accuracy of temperature-dependent systems in a wide range of operating conditions.

In this brief, we present a BJT-based CMOS temperature sensor that includes a BJT front-end designed for improved accuracy and performance which can generate the proportional to absolute temperature (PTAT) voltage  $V_{PTAT}$  and the complementary to absolute temperature (CTAT) voltage  $V_{CTAT}$ , these temperature-dependent voltages are then proceeded by a voltage-to-duty-cycle converter that can work with low voltage, this means that we reduce the supply voltage from 1.8V to 1.5V. In this sensor, an integrator is added to use a Schmitt trigger with larger hysteresis to have better noise immunity and design the sensor with a power supply of 1.5V. The proposed sensor has an inaccuracy of about  $\pm 0.11$  (from  $-55^{\circ}\text{C}$  to  $130^{\circ}\text{C}$ ) and FOM resolution of about  $1.4\text{pJ. }^{\circ}\text{C}^2$  while maintaining a chip area of  $0.64\text{mm}^2$  and power consumption is about  $45\text{uW}$ . In a standard  $0.18\text{-}\mu\text{m}$  CMOS process.

## 2. Methods

### 2.1. Basic Design

In *Figure 1*, Under the control of a Schmitt trigger, a capacitor C is periodically charged by a current  $I_1$  up to a threshold voltage  $V_2$  and then discharged by a current  $I_2$  down to a threshold voltage  $V_1$  (*Figure 1 (a)*).

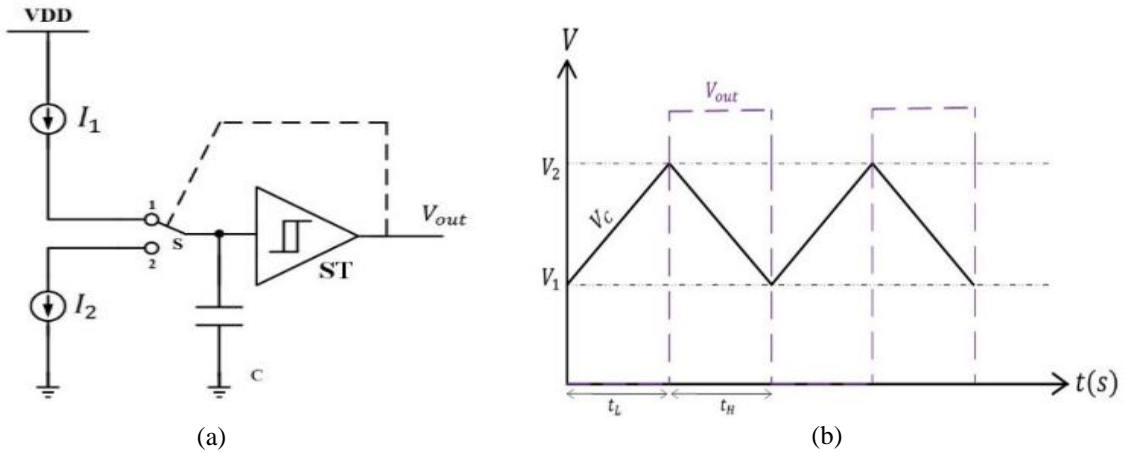


**Figure 1.** (a) basic circuit diagram; (b)  $V_C$  node voltage versus time and output voltage of Schmitt trigger versus time.

As can be deduced from the timing diagram shown in **Figure 1 (b)**, the duty-cycle of the resulting output signal equals (*Eq. (1)* and *Eq. (2)*) [7]:

$$\text{Duty Cycle} = \frac{T_H}{T_H + T_L} = \frac{\frac{V_C \cdot C}{I_1}}{\frac{V_C \cdot C}{I_1} + \frac{V_C \cdot C}{I_2}} \quad (1)$$

$$\text{Duty Cycle} = \frac{I_1}{I_1 + I_2} \quad (2)$$

In **Figure 2** the base-emitter voltage of  $Q_3$  ( $V_{CTAT}$ ) produces Current in  $R_{CTAT}$  ( $I_2$ ), which decreases by increasing the temperature. The difference between the base-emitter voltages of  $Q_1$  and  $Q_2$  ( $\Delta V = V_{BE1} - V_{BE2}$ ), which increases with temperature ( $V_{PTAT}$ ), produces current in  $R_{PTAT}$  ( $I_1$ ). The op-amp employs a folded-cascode topology, which achieves more than 80-dB dc-gain over process and temperature variations and its offset is mitigated by chopping. In this circuit, the capacitor of node A is charged once by the input current ( $I_1$ ) to this node and discharged once by the output current ( $I_2$ ) from this node. VA at different temperatures can be up to  $V_{dd} - 2V_{on}$  during the charging time of the capacitor and during discharge time, the  $V_A$  can reach up to 0.9 ( $V_{BE \text{ max}} + V_{on}$ ).  $V_{BE \text{ max}}$  occurs at a temperature of -55. That is, the range of Schmitt trigger input voltage changes will be (0.9-1.5) when  $V_{dd} = 1.8V$ .

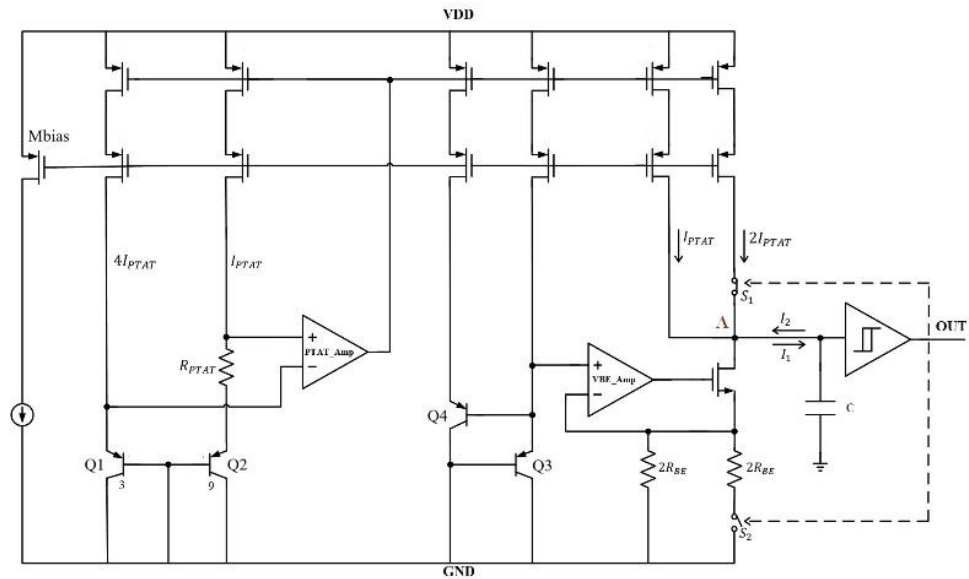


Figure 2. Temperature sensor circuit.

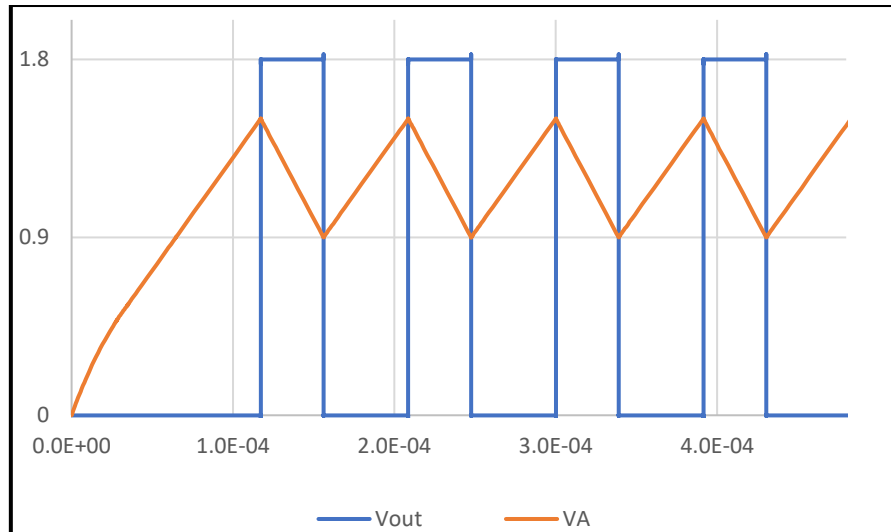


Figure 3.  $V_A$  variation range.

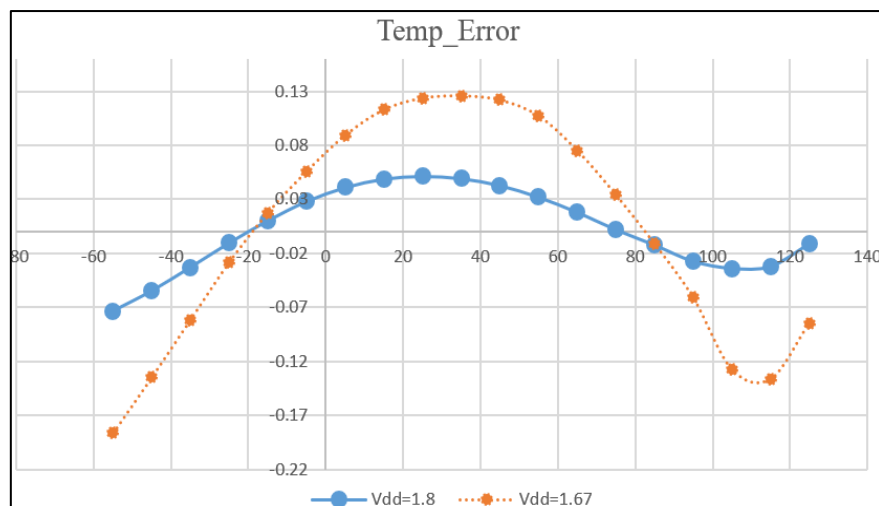


Figure 4. Voltage dependency of accuracy before adding an integrator.

## 2.2. Reduce Supply Voltage

According to the explanation in the previous paragraph if the Schmitt trigger hysteresis is chosen between 0.9 and 1.5 and the supply voltage ( $V_{dd}$ ) is less than the desired value during the manufacturing process due to mismatch effects, the current mirror's transistors enter the triode region which causes a decrease in the output resistance of the current sources and this effect decreases the current generated of current sources and affects the operation of the sensor and reduces the measurement accuracy. To evaluate the impact of device mismatch in fabricated integrated circuits, statistical simulation methods can be employed during the design phase. One widely used approach is the Monte Carlo simulation, which introduces random variations to the electrical parameters of circuit elements, such as threshold voltage, mobility, or resistor values, based on process variation models. This technique enables designers to statistically analyze circuit performance under realistic manufacturing conditions, allowing for a better understanding of yield, robustness, and functional reliability prior to fabrication. By simulating a large number of random instances, the Monte Carlo method helps identify worst-case scenarios and performance distributions, thereby guiding design optimization for improved tolerance to mismatch and process. In this case, Monte Carlo simulations show that the supply voltage generated for the temperature sensor block can be reduced to 1.67 V due to mismatch, while we expect this voltage to be 1.8 V. Error simulations for the sensor without an integrator show that changing the supply voltage from 1.8 to 1.67 V has a large impact on the sensor accuracy (*Figure 4*). However, simulations show that this voltage dependence is greatly reduced after adding the integrator block (*Figure 8*).

By adding the integrator in this node,  $V_A$  always will be constant and equal to the reference voltage of the integrator, and the voltage changes of this point will be transferred to the Schmitt trigger input by the integrator.

In order to use this temperature sensor in low voltage applications such as applications that a battery can be used as a power supply, it has been tried to reduce the sensor power supply from 1.8V to 1.5V.

## 2.3. Increase Accuracy and Resolution

During the initial design of the sensor architecture, prior to reducing the supply voltage from 1.8 V to 1.5 V, several accuracy-enhancement techniques were implemented. Specifically, dynamic element matching (DEM) was applied to minimize mismatch effects in current mirrors, while chopping was employed to suppress input offset in the amplifier [7], thereby ensuring higher measurement precision.

After decreasing the supply voltage to 1.5V, according to the points stated in section II, the Schmitt trigger's hysteresis can be only 0.3 V, and from what we know, small hysteresis in the Schmitt trigger can affect the noise immunity of the temperature sensor. To reduce the noise contribution of the Schmitt trigger, the hysteresis( $\Delta V = V_{LH} - V_{HL}$ ) will be increased [8].

If

$$V_{in}(t) = V_{signal}(t) + N(t) \quad (3)$$

$V_{signal}(t)$ : main signal

$N(t)$ : Noise added to the signal

And:

$$-\mathcal{E} < N(t) < \mathcal{E} \quad (4)$$

The condition that the noise does not affect the switching of the Schmitt trigger is:

$$\mathcal{E} < \Delta V \quad (5)$$

So, with a larger  $\Delta V$ , the noise contribution of the Schmitt trigger will be less. In this case, the headroom of the current mirrors is greatly reduced, so it is necessary that the voltage of node A does not exceed the virtual limit. Therefore, by adding an integrator, we fix the voltage of node A to a constant value.

In this situation, this goal can be achieved by using a wide- range Schmitt trigger because the input of the integrator is fixed, but its output can change within the swing of the integrator output.

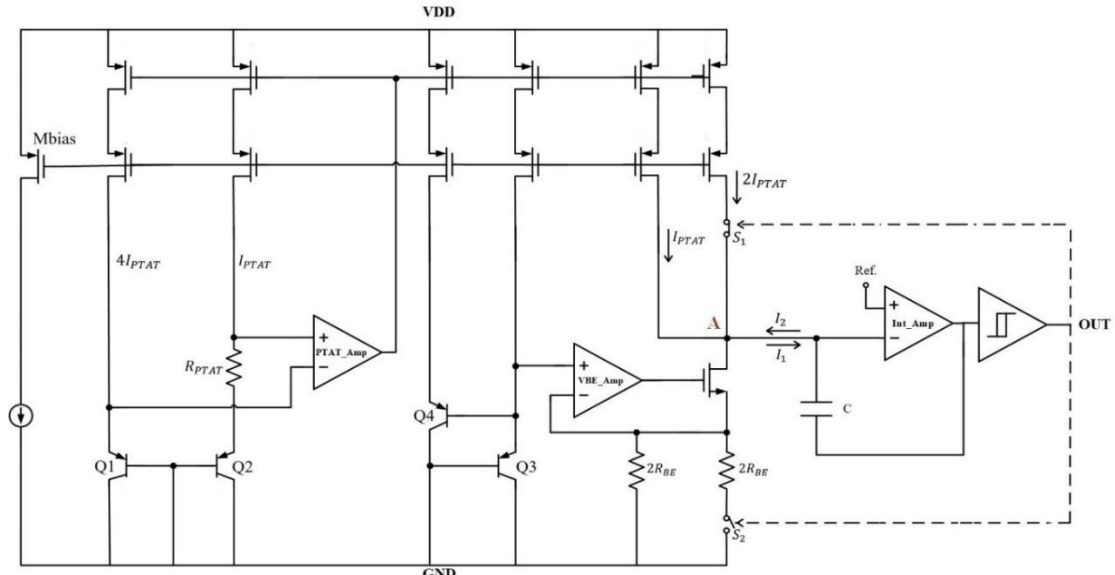


Figure 5. Temperature sensor circuit with integrator.

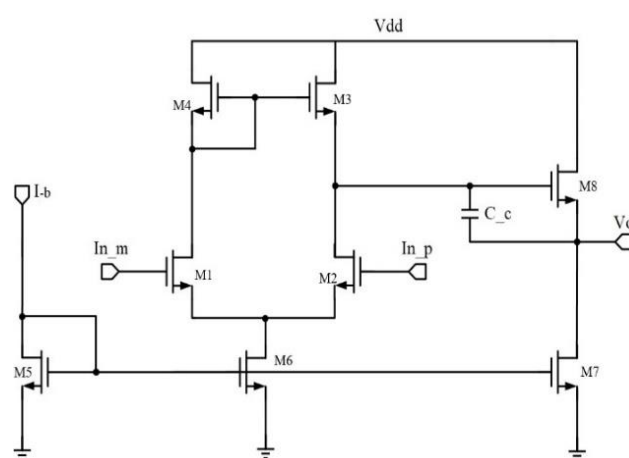


Figure 6. Integrator circuit.

According to **Figure 7**, A two-stage Op-amp is selected as an integrator and the output swing of this integrator will be ( $V_{on7} < out < V_{dd} - V_{on8}$ ). in this sensor  $V_{dd}$  is considered 1.5V. So, the Schmitt trigger's input variation range will be between (0.2-1.3) and switching voltages  $V_{LH}$  and  $V_{HL}$  can be selected as **Eq. (6)** and **Eq. (7)**:

$$V_{LH} = V_{dd} - V_{on} \quad (6)$$

$$V_{HL} = V_{on} \quad (7)$$

In designing the amplifier as an integrator used in this structure, it is important that the output stage of the amplifier has the capability to source and sink the current necessary to charge and discharge the capacitor (C).

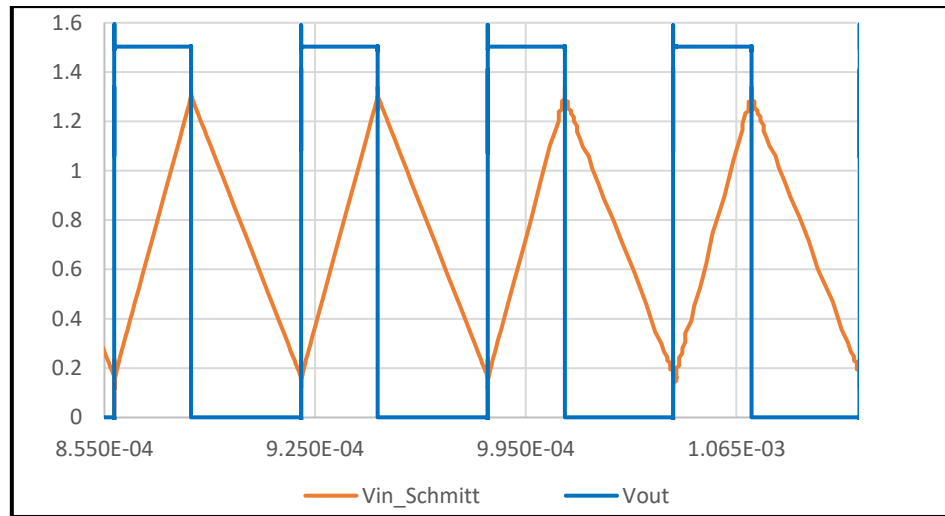


**Figure 7.** Schmitt triggers input variation range after adding the integrator.

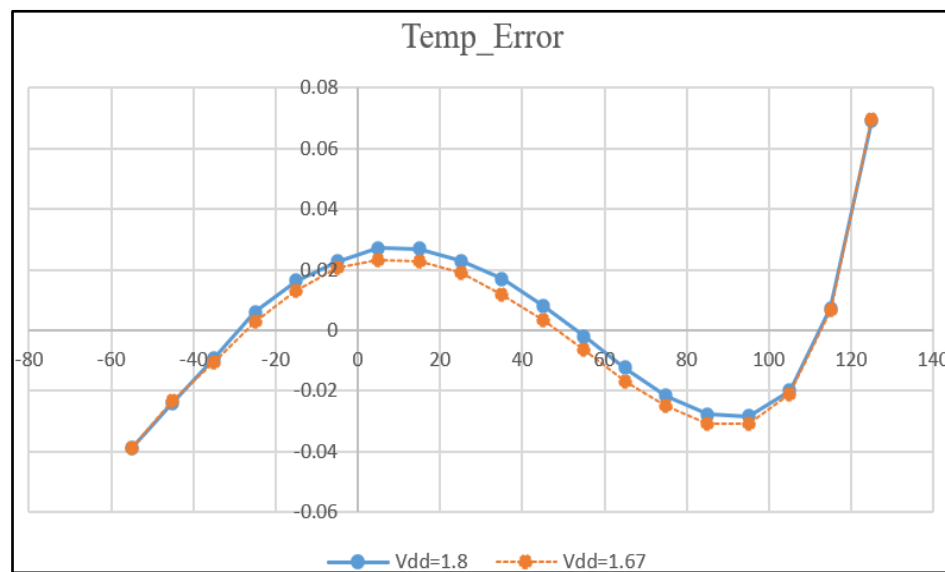


**Figure 8.** Voltage dependency of accuracy after adding an integrator.

### 3. Result

The proposed temperature sensor was fabricated using a standard 0.18- $\mu\text{m}$  CMOS process and occupies an active die area of 0.64 mm<sup>2</sup>. A die photograph of the complete system, including the integrated temperature sensor, low-dropout regulator (LDO), and reference generator, is shown in *Figure 9(a)*.

To evaluate the accuracy and performance of the sensor, 16 fabricated samples were characterized across a wide temperature range. Measurements were conducted in a temperature-controlled oven, as illustrated in *Figure 9(b)*, covering temperatures from  $-55^{\circ}\text{C}$  to  $+130^{\circ}\text{C}$ . The resulting temperature inaccuracy across all measured dies is plotted in *Figure 10*.

After applying a one-point calibration, the sensor achieves a maximum inaccuracy of  $\pm 0.11^{\circ}\text{C}$  ( $3\sigma$ ) over the full temperature range, as depicted in *Figure 11*.

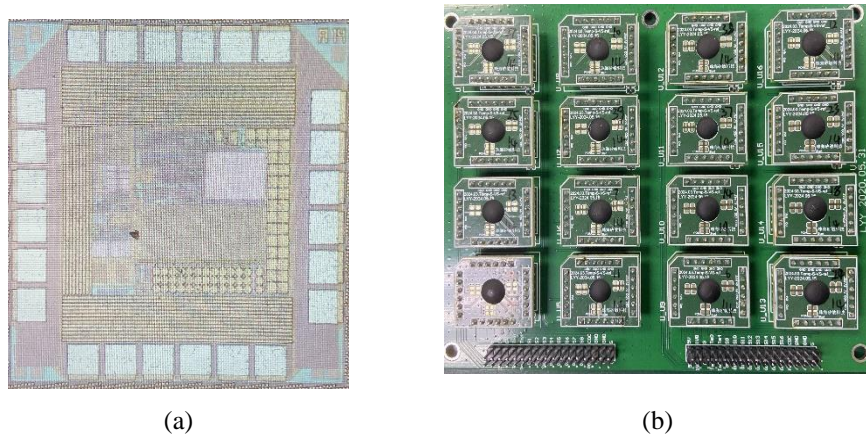


**Figure 9.** (a) Photograph of smart temperature sensor. (b) sensors in PCB

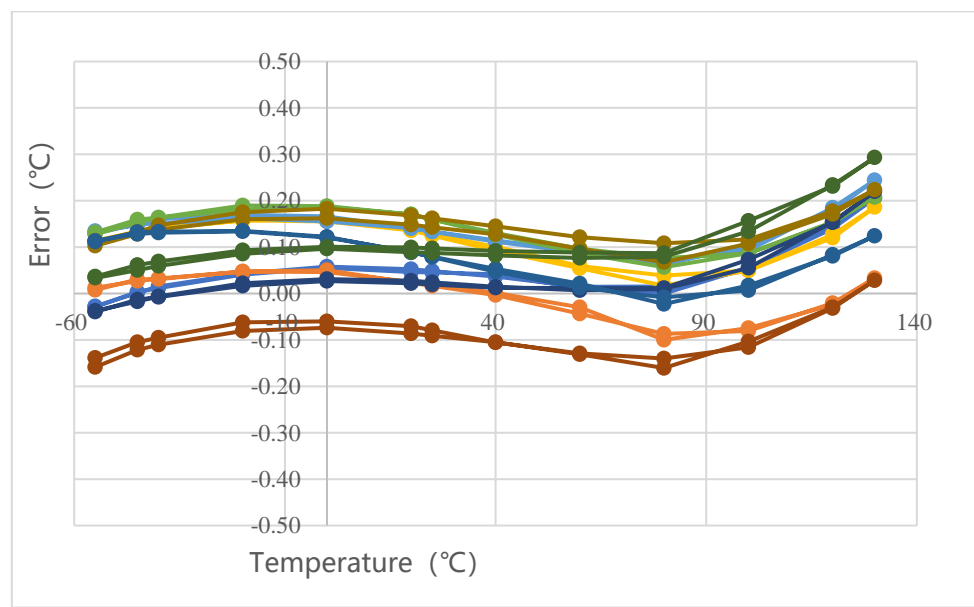


**Figure 10.** Measured inaccuracy.

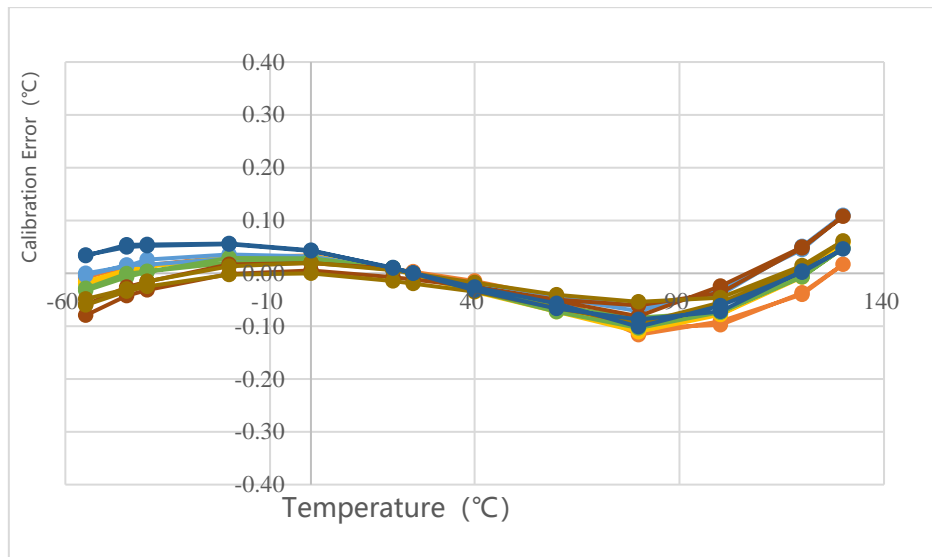


**Figure 11.** Measured inaccuracy after 1-point calibration.

#### 4. Discussion

These results confirm that the sensor delivers excellent thermal linearity and robustness, demonstrating its suitability for high-precision temperature monitoring in energy-constrained and noise-prone environments.

**Table 1** presents a comparative analysis between the proposed temperature sensor and prior works reported in [7], [9], and [10].

**Table 1.** Performance summary and comparison with BJT-based temperature sensors

Reference	This work	[7]	[9]	[10]
Technology(µm)	0.18	0.7	0.18	0.18
sensor type	BJT	BJT	BJT	BJT
ADC	DC <sup>1</sup>	DC	DC	DC
Temperature Range (°C)	-55–130	-45–130	-40–125	-50–180
Area (mm <sup>2</sup> )	0.64	2.21	0.35	0.42
Inaccuracy(°C)	0.11	0.3	0.13	0.45
Supply (V)	1.5–2	2.7–5.5	1.6–2.2	1.5–2
Power (µW)	45	198	9	3.8
Resolution (mk)	5	3	1.67	17.6
Resolution FOM (pJ. k <sup>2</sup> )	1.4	3.2	5.4	9.7
conversation time (ms)	1.3	1.8	218	8.3

1.Duty Cycle

2.Resolution FOM = power. Conversion time. (Resolution)<sup>2</sup>

## 5. Conclusion

A low-voltage CMOS temperature sensor with a duty-cycle-modulated (DCM) output has been presented, featuring a high energy efficiency and precise thermal performance. The sensor achieves a figure-of-merit (FOM) resolution of approximately  $1.4 \text{ pJ}/\text{°C}^2$ , enabled by incorporating an input-stage integrator and using the Schmitt trigger with larger hysteresis. These architectural improvements contribute to enhanced resolution without significantly increasing power consumption or area. The sensor operates reliably with a 1.5 V supply and exhibits a measured inaccuracy of  $\pm 0.11 \text{ °C}$  ( $3\sigma$ ) over a wide temperature range from  $-55 \text{ °C}$  to  $130 \text{ °C}$ . Fabricated in a standard  $0.18\text{-}\mu\text{m}$  CMOS process, the design occupies an active silicon area of  $0.64 \text{ mm}^2$ . The total power consumption is approximately  $45 \text{ }\mu\text{W}$ , making the sensor well-suited for deployment in low-power applications such as wearable electronics, wireless sensor nodes, and energy-harvesting systems.

## References

- [1] Zhong Tang, Sining Pan, Miloš Grubor, and Kofi A. A. Makinwa (2023). A Sub-1 V Capacitively Biased BJT-Based Temperature Sensor with an Inaccuracy of  $\pm 0.15 \text{ °C}$  ( $3\sigma$ ) From  $-55 \text{ °C}$  to  $125 \text{ °C}$ . *IEEE JOURNAL OF SOLID-STATE CIRCUITS*.
- [2] R. Zhang, S. Fan, and L. Geng (2018). A near-zero-power temperature sensor with  $\pm 0.24 \text{ °C}$  inaccuracy using only standard CMOS transistors for IoT applications. *IEEE ISCAS*, 1–4.
- [3] K. Makinwa (2020). Smart temperature sensor survey. <http://ei.ewi.tudelft.nl/docs/TSensor survey.xls>.
- [4] Nandor G. Toth, Zhong Tang, Teruki Someya, Sining Pan, Kofi A. A. Makinwa (2023). A BJT-Based Temperature Sensor with  $\pm 0.1\text{°C}$  ( $3\sigma$ ) Inaccuracy from  $-55\text{°C}$  to  $125\text{°C}$  and a  $0.85\text{pJ}\cdot\text{K}2$  Resolution FoM Using Continuous-Time Readout. *IEEE International Solid-State Circuits Conference*.
- [5] B. Yousefzadeh and K. A. A. Makinwa (2017). 9.3 A BJT-based temperature sensor with a packaging-robust inaccuracy of  $\pm 0.3 \text{ °C}$  ( $3\sigma$ ) from  $-55 \text{ C}$  to  $+125 \text{ °C}$  after heater-assisted voltage calibration. *ISSCC*, 162–163.
- [6] Bahman Yousefzadeh, and Kofi A. A. Makinwa (2020). A BJT-Based Temperature-to-Digital Converter With a  $\pm 0.25 \text{ °C}$   $3\sigma$ -Inaccuracy From  $-40 \text{ °C}$  to  $+180 \text{ °C}$  Using Heater-Assisted Voltage Calibration. *IEEE JOURNAL OF SOLID-STATE CIRCUITS*, 55(2).
- [7] G. Wang, A. Heidari, K. A. A. Makinwa, and G. C. M. Meijer (2017). An accurate BJT-based CMOS temperature sensor with duty-cycle modulated output. *IEEE Trans. Ind. electron.*, 64(2), 1572– 1580.
- [8] Rajendar Sandiri, Yashwanth Chimata, Yashwanth Nalamasa, Pavan Arra (2022). Design of Noise Immune Subthreshold Circuits using Dynamic Threshold Schmitt Trigger Logic. *IEEE Region 10 Symposium (TENSYMP)*.
- [9] R. K. Kumar, H. Jiang, and K. A. A. Makinwa (2019). An energy-efficient BJTbased temperature-to-digital converter with  $\pm 0.13\text{°C}$  ( $3\sigma$ ) inaccuracy from  $-40$  to  $125\text{°C}$ . *IEEE Asian Solid-State Circuits Conf. (A-SSCC)*, 107–108.
- [10] Bo Wang and Man-Kay Law (2022). Subranging BJT-Based CMOS Temperature Sensor With a  $\pm 0.45 \text{ °C}$  Inaccuracy ( $3\sigma$ ) From  $-50 \text{ °C}$  to  $180 \text{ °C}$  and a Resolution-FoM of  $7.2 \text{ pJ}\cdot\text{K}2$  at  $150 \text{ °C}$ . *IEEE JOURNAL OF SOLID-STATE CIRCUITS*, 57(12).